A mechanism of chute cutoff along large meandering rivers with uniform floodplain topography

José Antonio Constantine[1,*], Stephen R. McLean[2], and Thomas Dunne[1,3]
[1]*Department of Earth Science, University of California–Santa Barbara, Santa Barbara, California 93106, USA*
[2]*Department of Mechanical Engineering, University of California–Santa Barbara, Santa Barbara, California 93106, USA*
[3]*Donald Bren School of Environmental Science and Management, University of California–Santa Barbara, Santa Barbara, California 93106, USA*

ABSTRACT

Incidents of chute cutoff are pervasive along many meandering rivers worldwide, but the process is seldom incorporated into theoretical analyses of planform evolution, partly due to the paucity of observations describing its physical controls. Here, we describe a mechanism of chute cutoff that may be prevalent along large meandering rivers with uniform floodplain topography. The mechanism occurs independently of sudden changes in conveyance capacity, such as those caused by natural dams, and instead, it is initiated during a flood by the incision of an embayment. The embayment is typically located almost a channel width upstream of the entrance to the meander that undergoes cutoff, and subsequent floods extend the embayment downstream until a chute is formed. Using sequences of historical aerial photos of the Sacramento River in California, USA, we found that embayments formed where channel curvature was greatest, or where the channel most tightly curved away from the downstream flow path. Embayments formed only within those portions of the floodplain that were lightly vegetated by grasses or crops. We develop a simple physical model that describes the environmental conditions that can lead to embayment formation. The model considers the role of floodplain vegetation in preventing chute incision and in part explains why chute cutoff is prevalent along some meandering rivers but not others.

INTRODUCTION

Meander cutoff is a fundamental process in the evolution of meandering rivers. As the meandering river gradually increases the space it occupies in the floodplain by the growth of meander bends, incidents of cutoff shorten the river's length and produce oxbow lakes that create topographic diversity and sediment sinks in the floodplain (Lauer and Parker, 2008; Aalto et al., 2008). Although two cutoff processes are commonly recognized (Lewis and Lewin, 1983; Gagliano and Howard, 1984), planform evolution models typically only incorporate neck cutoff (e.g., Howard, 1992; Stølum, 1998; Camporeale et al., 2005), a process that results from bank collapse after maturing meanders have migrated into one another (Gagliano and Howard, 1984; Hooke, 1995). The second cutoff process occurs when floods incise a floodplain channel, or chute, that evolves into the dominant conveyor of river discharge (Hooke, 1995; Gay et al., 1998). Termed chute cutoff, this process has been recognized as a major control on the planforms of actively meandering rivers because its occurrence prevents meanders from maturing into long segments of channel, thereby limiting a river's sinuosity. The exclusion of chute cutoff in the development of theory explaining meandering behavior is partly due to the difficulty of incorporating the process within current models of long-term meandering and partly due to the paucity of observations describing the physical controls on chute cutoff across a range of natural settings. In the absence of such observations of the process, the importance of chute cutoff to the evolution of the meandering planform is difficult to analyze physically, and the only means of examining the effects of chute cutoff on meandering behavior is by treating it as quasi-random in heuristic models (e.g., Howard, 1996).

Floods initiate flow over the floodplain wherever local water heights exceed bank elevations; this is not necessarily an issue during large flood stages, but it is also not trivial during small flood stages given any variability in bank topography. Chutes are then eroded into the floodplain whenever floods have enough energy to transport sediment from the floodplain floor, as well as any sediment delivered from the river, out of the floodplain and back into the river. The energy of a flood is reflected in the slope of the flood's water surface—the more steeply sloping the water surface, the greater the potential and kinetic energy of the flood. Local differences in the shape of the floodwater surface will determine the particular means by which a chute is eroded. Any number of environmental conditions on the floodplain (e.g., local differences in topography, sediment composition, and vegetation) can alter the floodwater surface in such a way as to promote or inhibit erosion, and so it is reasonable to expect that characteristics of chute incision may vary considerably between settings. Indeed, a precise understanding of how chute cutoff occurs will stem only from a detailed examination of the hydraulic controls on chute incision, not from an empirical analysis of environmental variables. Nonetheless, typical mechanisms of chute incision have been recognized in the field, and a description of the field conditions that lead to each mechanism will do much to improve our understanding of the systematic differences in chute cutoff observed across a range of natural settings as well as aid attempts to successfully manage and restore the dynamics of meandering rivers.

At least three different mechanisms of chute cutoff have been recognized in nature. The first mechanism was qualitatively described by Fisk (1947) along the Lower Mississippi River, as well as by Bridge et al. (1986) along the Calamus River of Nebraska, USA, and it is evident along many meandering rivers that develop pronounced ridge and swale, or scroll bar, topography (see Hickin and Nanson, 1975). Swales within the floodplain can function to channelize overbank flow (Fig. 1). In cases where a particular swale provides the predominant flood routing path, gradual erosion may enlarge the swale until it forms a channel conveying most of the discharge, thereby causing chute cutoff. The development of chutes by swale enlargement may be commonplace, but

*E-mail: constantineja@cardiff.ac.uk; current address: School of Earth and Ocean Sciences, Cardiff University, Cardiff CF10 3YE, UK.

GSA Bulletin; doi: 10.1130/B26560.1; 16 figures; 2 tables; Data Repository item 2009210.

Figure 1. Floodplain channels within an Amazonian floodplain. Such channels provide efficient conduits for overbank flow and, under certain conditions, may be enlarged enough to cause chute cutoff. Photograph by T. Dunne.

a characterization of this mechanism over time scales of significant meander migration will require an improved physical understanding of scroll bar formation.

The second mechanism of chute cutoff involves the formation of a natural dam that locally forces water overbank and across the floodplain. As a result of the stage difference upstream and downstream of the natural dam, the returning flow plunges over the riverbank and back into the channel. The plunging water can result in bank incision, creating a headcut that propagates upstream until it forms a chute (Fig. 2). Chute cutoff by headcut extension has been observed by at least three studies. Keller and Swanson (1979) observed that the piling up of woody debris within narrow (<50 m) streams of North Carolina forced flow overbank and resulted in chute cutoff. Gay et al. (1998) documented how the piling up of ice at several positions forced flow overbank, leading to chute incision by headcut extension along the narrow (<50 m) Powder River of Montana. Thompson (2003) observed a similar mechanism along the narrow (<25 m) Blackledge River of Connecticut. As a result of localized bed aggradation along a meander, the conveyance of the channel was reduced, and flow was forced overbank, resulting in headcut extension and chute cutoff. Although a cohesive floodplain is likely required to maintain the form of the headcut (Brush and Wolman, 1960), the studies imply that chute cutoff by headcut extension may be common along narrow meandering streams where flow can be locally forced overbank. Physical theory has not been explicitly developed to describe chute cutoff by headcut extension, but research on the formation of gullies and rills by headcut erosion (e.g., Alonso et al., 2002; Stein and LaTray, 2002) may provide the foundation from which chute cutoff by this mechanism can be fully understood.

We report a third mechanism of chute cutoff along large meandering rivers with relatively uniform floodplain topography. At least in the modern era, most large rivers in midlatitudes are devoid of natural dams, and in these rivers, the controls on chute cutoff independent of sudden changes in conveyance capacity have not been previously described. Observations along the wide (>200 m) Sacramento River of California (Fig. 3) and the wide (>200 m) Missouri River of the central Unites States (Fig. 4) indicate that chute incision along these kinds of rivers can occur by the downstream extension of an embayment. The embayments appear to be a result of localized bank erosion along the outer bank of the channel located upstream of the meander that undergoes cutoff. Subsequent floods extend the embayment, shifting it downstream by floodplain erosion until it intersects the

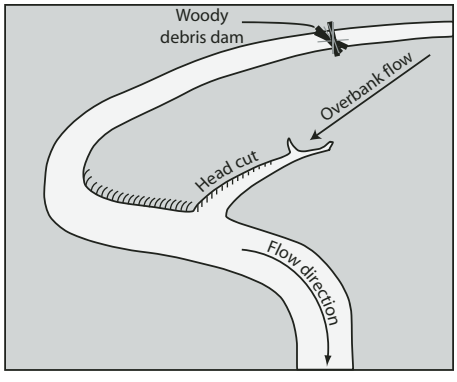

Figure 2. Schematic illustrating the formation of a headcut caused by flooding due to a natural dam. The stage difference upstream and downstream of the dam causes returning overbank flow to plunge across the riverbank, forcing the extension of the headcut. Headcut extension by this mechanism has been identified as a cause of chute cutoff within narrow streams.

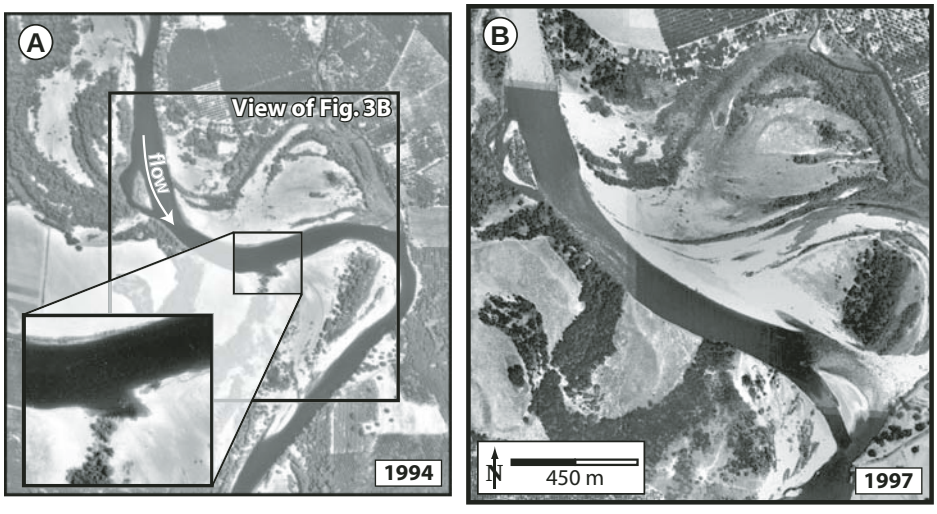

Figure 3. (A) Aerial photo of a meander near river kilometer 377 of the Sacramento River taken in 1994. Enlargement shows a section of the outer bank where an embayment existed. (B) Aerial photo of the same location in A taken in 1997. Between 1994 and 1997, the embayment shown in A became the entrance location of a chute. The modern chute can be seen using Google Earth™ by navigating to 40.095°N, 122.115°W.

riverbank downstream, thereby forming a chute. Markham and Thorne (1992) described the formation of embayments along the River Roding, UK, but the physical controls on embayment formation were not examined. Hauer and Habersack (2009) also described embayments along the Kamp River, Austria, and they attributed embayment formation to the hydraulic effects of sudden increases in valley width during a large flood event. The Sacramento and Missouri Rivers naturally have wide valleys (>20 channel widths) that do not rapidly vary in width, and so an alternative explanation of embayment formation is needed for such rivers.

In the present work, we examine the physical controls on chute incision by embayment formation and extension, possibly the dominant mechanism of chute cutoff along large meandering rivers with uniform floodplain topography. We focus on the Sacramento River where a historical record of aerial photographs allowed us to examine the mechanism in detail. We attempt to explain the locations of embayment formation by characterizing flood conditions along an actively meandering reach of the river using a two-dimensional hydrodynamic model. Observations from aerial photographs and computer modeling are generalized by developing a simple physical model of the environmental conditions required for embayment formation. Although the model does not consider incision of the entire chute, it provides a theoretical basis for explaining the absence of chute cutoff along many meandering rivers and its predominance along others. By identifying the physical controls on chute cutoff by embayment formation, our work contributes to efforts to incorporate chute cutoff into theoretical models of meandering rivers and clarifies where more detailed hydraulic studies of the conditions favoring chute cutoffs might be targeted.

PHYSICAL SETTING

The 68,000 km^2 watershed of the Sacramento River drains the crystalline Sierra Nevada and Klamath Mountains, the sedimentary formations of the Great Valley and Coast Ranges, and the southern end of the volcanic Cascade Range and Modoc Plateau (Norris and Webb, 1976) (Fig. 5). For study, we selected a 160-km-long reach of the river with freely migrating meanders that are well connected to the surrounding floodplain and divided the reach into an upper and a lower segment based on differences in channel characteristics (Fig. 5; Table 1). Since 1945, average annual discharge has ranged from 350 m^3 s^{-1} near Red Bluff, California (U.S. Geological Survey [USGS] gauge 11377100), to 330 m^3 s^{-1} near Colusa, California (USGS gauge 11389500) (Fig. 5), from precipitation between 50 and 178 cm a^{-1} (Buer, 1994). Channel-altering floods usually occur in response to large winter rainstorms and rapid melting of the Sierra Nevada snowpack, but since 1945, these floods have been regulated to varying degrees by several large reservoirs. For example, flow regulation has reduced the 2 and 10 a annual maximum discharges near Red Bluff (Fig. 5) from 3300 and 5800 m^3 s^{-1}, respectively, to 2100 and 3800 m^3 s^{-1} (USGS gauge 11377100), respectively. Long-term average bed-load transport in the reach varies along the river's course from 0.1 to 1.0 Mt a^{-1} (Singer and Dunne, 2004a), and suspended load (65% of which is finer than 0.063 mm) averages 12 Mt a^{-1} (USGS gauge 11389500), although this estimate of suspended load may be declining in light of findings that sediment concentrations have been reduced since flow regulation (Wright and Schoellhamer, 2004). The bed material of the Sacramento River includes particles from 128 mm down to silt and clay, but particles finer than 0.5 mm typically make up only 20%–40% of the total bed material, even though suspended load is dominated by this grain size (Singer, 2008, their figure 2).

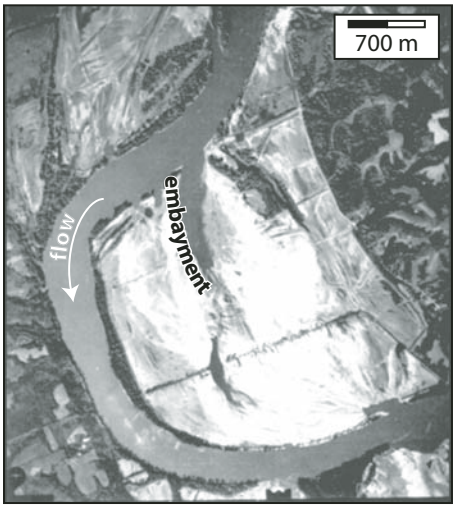

Figure 4. Aerial photo of a reach of the Missouri River taken after a large flood in 1993 showing a floodplain embayment that was gradually extended downstream until forming a chute. The modern chute can be seen, as well as the engineering structures put in place to prevent chute cutoff, using Google Earth™ by navigating to 39.115°N, 92.925°W. Photo is courtesy of the U.S. Geological Survey.

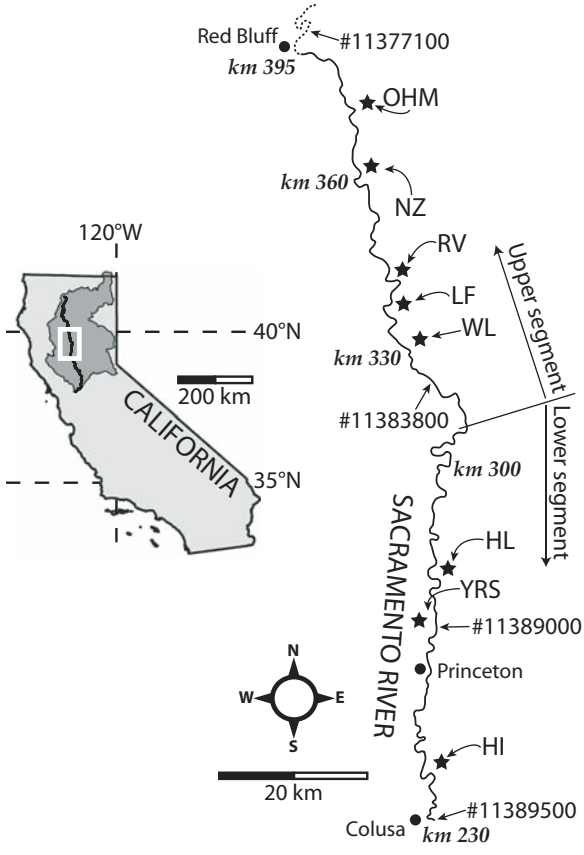

Figure 5. Location maps of the Sacramento River watershed and the study reach between the cities of Red Bluff and Colusa. The approximate locations of gauges, from which recorded data were used in the study, are shown by the #'s. Dashed lines represent the segments of river that are outside the study reach but that have a nearby U.S. Geological Survey (USGS) gauge. Stars illustrate the approximate locations of chute cutoff events examined in the study, and the bold italicized numbers (e.g., km *230*) indicate the locations of river kilometers.

TABLE 1. STUDY REACH CHARACTERISTICS OF THE SACRAMENTO RIVER

Reach segment	Upper	Lower
River kilometers	391 to 311	311 to 230
Sinuosity	1.33	1.50
Bankfull discharge ($m^3 s^{-1}$)*	1780	1620
Average bankfull width (W) (m ±1σ)*	259 (±109)	246 (±60.7)
Average bankfull depth (y) (m ±1σ)*	5.45 (±1.37)	5.68 (±1.24)
Bankfull, reach averaged downstream flow velocity (U) ($m s^{-1}$ ±1σ)*	1.76 (±0.35)	1.29 (±0.28)
Average bed slope (S)	5.40×10^{-4}	2.80×10^{-4}
Dimensionless friction coefficient (C_f)	0.0093	0.0094
Scour factor (A) (±2σ)†	2.52 (±1.1)	4.14 (±0.62)

*Determined from HEC-RAS simulations using U.S. Army Corps of Engineers and U.S. Geological Survey (USGS) cross-section data.

†Determined after Pizzuto and Meckelnburg (1989) using U.S. Army Corps of Engineers and USGS cross-section data.

The banks of the Sacramento River range from cohesive or cemented material to coarse, noncohesive alluvium. In general, the upper 3 m of the floodplain consist of sand and silt, below which, floodplain sediment coarsens to sand and gravel (recorded in borings retrieved by the California Department of Transportation). Sediment samples from the tops of outer banks near river kilometers 276 and 320 have median particle diameters (d_{50}) of 0.063 and 0.13 mm and 84th percentile particle diameters (d_{84}) of 0.11 and 0.22 mm. The California Department of Water Resources (1979) reported that the d_{84} of surficial bank sediment ranged between 0.08 and 0.17 mm between river kilometers 233 and 303. Scroll bars and other features that would enhance the variability of floodplain topography are generally absent. Floodplain vegetation is densest along the perimeters of the river and oxbow lakes, consisting of woodland species in the riparian corridor and grassland species in much of the remaining floodplain (Buer, 1994). Land use has altered the composition of floodplain vegetation in some places by the introduction of orchards and other types of crop farming.

HISTORICAL INCIDENTS OF CHUTE INCISION

We identified ten incidents of chute cutoff within the study reach of the Sacramento River using a record of digitized and georeferenced historical aerial photos spanning the period from 1938 to 2004. For each incident, we digitized a channel centerline using the latest photo preceding incision and recorded the location of the chute entrance relative to 50-m-spaced centerline points. We smoothed each set of centerline points and calculated local curvature (α), and its inverse, the local radius of curvature (r), along centerline points after Fagherazzi et al. (2004). The presence or absence of vegetation in the vicinity of each identified chute was documented, as well as the form of floodplain vegetation (i.e., trees, shrubs, and grasses). We determined the largest mean daily discharge during the time span in which each chute was incised as recorded by the nearest U.S. Geological Survey (USGS) gauge.

The chutes ranged in length from 2.4 to 16.1 channel widths and averaged 10.4 ± 4.8 channel widths (Table 2). The ratio of the chute length to the removed meander length ranged from 0.32 to 0.68 and averaged 0.48 ± 0.13. The maximum mean daily flood discharge during the time span that each chute was incised ranged from 2073 to 7391 $m^3 s^{-1}$, or ~1.2–4.3 times the bankfull discharge (Table 2). Given the temporal gaps within the record of aerial photos, we were unable to document stages of chute incision. At five of the historical locations, however, we observed that an embayment existed in the outer bank (the bank toward which surface flows are advected due to centripetal motion) prior to incision and at the entrance to each future chute (Figs. 3 and 6). We also observed that, in each case, incision occurred in portions of the floodplain that were either lightly vegetated by grasses or farmed (Fig. 6).

We recognized three additional characteristics of floodplain incision within each of the chute-producing reaches. First, each chute entrance occurred upstream and in the vicinity of the inflection, or crossover, of the meander that underwent cutoff (Fig. 7). The upstream distance between the inflection and the chute entrance ranged from 0.4 to 2.1 channel widths and averaged 0.98 ± 0.60 channel widths, comparable to observations by Lewis and Lewin (1983), who quantified the location of chute entrances along rivers in Wales and the Welsh Borderlands, but who did not offer a physically based explanation for cutoff locations. Second, chute entrances generally occurred at the most tightly curved part of the channel just upstream of the inflection of the meander that underwent cutoff (Fig. 7). The local radius of curvature at each chute entrance ranged from 0.56 to 1.4 channel widths and averaged 0.81 ± 0.24 channel widths. This finding is also comparable to that of Lewis and Lewin (1983), who found that most chutes were incised at locations where the radius of curvature was less than 3 channel widths. A small chute was incised at river kilometer 328 where channel curvature was greatest (Fig. 6), but the chute that ultimately induced cutoff was subsequently incised at an upstream location that more closely paralleled the valley slope. Such a scenario might well have occurred at river kilometer 230 if not for the presence of a confining levee (Fig. 6). Third, the chute entrance path generally paralleled the upstream main channel path at each location, implying that a portion of the discharge was diverted from the main channel and followed a straight course into each chute.

THE ROLE OF CHANNEL CURVATURE

Changes in Curvature during Planform Evolution

The consistency of our findings, as well as their agreement with those of other workers, suggests that channel curvature of the upstream

TABLE 2. HISTORICAL INCIDENTS OF CHUTE INCISION ON THE SACRAMENTO RIVER

River (km)	Years*	Q_i ($m^3 s^{-1}$)	Q_i RI† (a)	Chute length (channel widths)	Length ratio§
230	1938–1958	4701#	45	8.4	0.52
269	1968–1974	4134#	7.8	2.4	0.46
282	1938–1947	4701#	45	11.9	0.68
282	1956–1974	4474#	23	9.8	0.33
328	1958–1974	4276**	23	11.2	0.34
338	1999–2004	2073††	1.6	3.07	0.50
344	1958–1974	4276**	13	14.0	0.32
367	1938–1956	7391††	60	11.2	0.53
377	1958–1994	3596††	7.5	16.1	0.47
377	1994–1997	3030††	4.0	16.1	0.68

*Time span during which a chute was incised. Years are based on the latest available photo before incision and the earliest available photo after incision.

†Recurrence interval (RI) for the maximum mean daily flood discharge (Q_i) shown in the preceding column during the post–1945 hydrologic regime.

§Ratio of chute length to the length of the removed meander.

#The maximum mean daily flood discharge based on the record of U.S. Geological Survey (USGS) gauge #11389000.

**The maximum mean daily flood discharge based on the record of USGS gauge #11383800.

††The maximum mean daily flood discharge based on the record of USGS gauge #11377100.

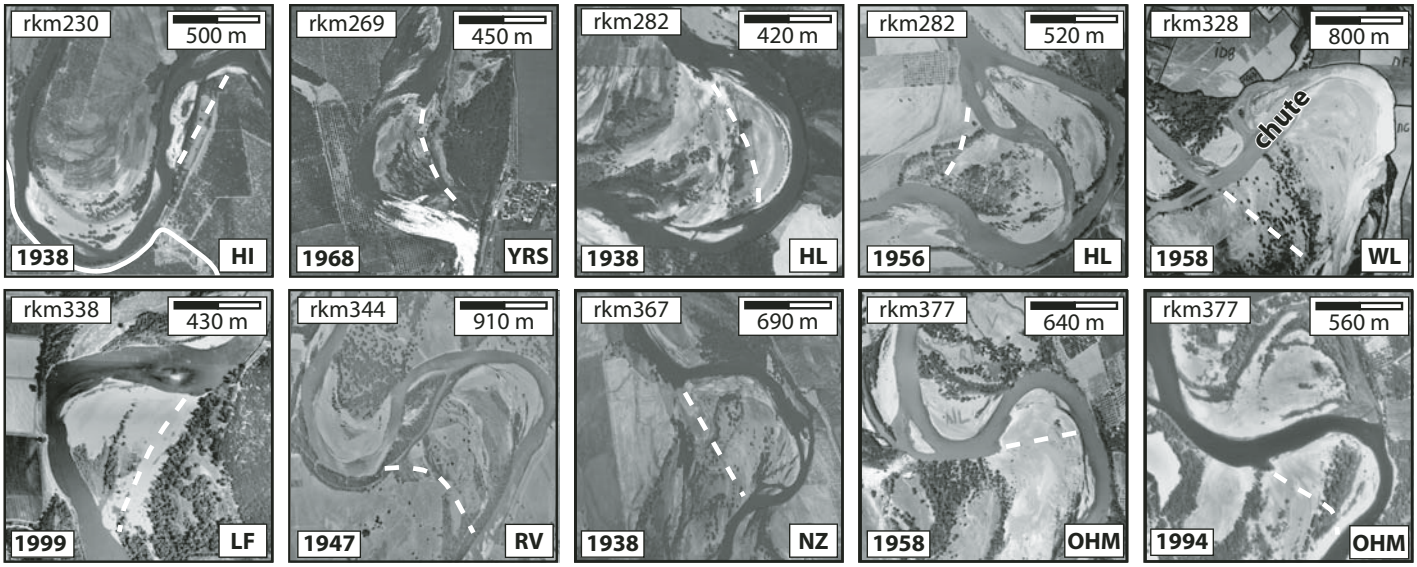

Figure 6. The 10 locations we identified as having experienced chute cutoff between 1938 and 2004. The photos shown are the latest available prior to chute incision. The date of each photo is provided as well as the approximate river kilometer (rkm) location along the Sacramento River. Dashed lines represent the locations of chutes that were incised. The flow direction in each case is from the top of the page. The solid white line drawn within *rkm230* illustrates the location of a levee. The location of each photo is shown in Figure 5 and can be found using the abbreviation provided in the bottom right corner of each photograph.

meander influences the location in which chutes are incised, at least in large rivers with relatively uniform floodplain topography. The implication then is that evolution of the meander planform controls the location of chute incision. Within a meander, curvature and shoaling of flow onto and over the point bar force high-momentum fluid to be advected radially outward (see Dietrich et al., 1979; Dietrich and Smith, 1983; Johannesson and Parker, 1988; Whiting and Dietrich, 1991). The result of this shoaling increases the pool depth, water-surface elevation, and flow velocity along the outer bank (Dietrich et al., 1979). The proximity of high-momentum fluid to the outer bank is thought to have an important control on rates of bank erosion (Leliavsky, 1966; Pizzuto and Meckelnburg, 1989). The basis of this hypothesis resides originally in empirical observations that bend migration rates vary with curvature (Hickin, 1974; Hickin and Nanson, 1975), appealing to the importance of higher shear stresses near the outer bank. This idea has been elaborated in models of meandering that assume that the migration rate varies with the near-bank flow velocity in excess of the section-averaged velocity (e.g., Ikeda et al., 1981; Johannesson and Parker, 1989; Odgaard, 1987; Pizzuto and Meckelnburg, 1989; Zolezzi and Seminara, 2001). For example, the linear theory of meander migration (see Ikeda et al., 1981) states that fluvial erosion of the outer bank (E_i) at any streamwise location i can be expressed as:

$$E_i = \varepsilon\omega_i, \tag{1}$$

where ε represents a dimensionless coefficient that reflects the erodibility of bank material, and ω_i is a near-bank velocity term equal to the difference between the reach-averaged velocity and the depth-averaged velocity near the outer bank. Micheli et al. (2004) quantified values of ε along farmed floodplains of the Sacramento River, and we use the average of their reported values, equal to 6.15×10^{-7} ($\pm 2.1 \times 10^{-7}$), as an estimate of ε. Sun et al. (1996, their Equation 15) calculated ω_i as:

$$\omega_i = \frac{b}{U/\Delta s_i + 2(U/y)C_f}\left[-U^2\left.\frac{\partial\alpha}{\partial s}\right|_i + C_f\alpha_i\left(\frac{U^4}{gy^2} + A\frac{U^2}{y}\right) + \frac{U}{\Delta s_i}\frac{\omega_{i-1}}{b}\right], \tag{2}$$

where b represents the average bankfull half-width of the channel, Δs_i represents the change in distance between centerline points, U represents the cross-sectionally averaged downstream flow velocity, y represents the average bankfull channel depth, C_f represents a dimensionless friction coefficient that we treat as a constant and equal to gyS/U^2 (where g is gravitational acceleration [9.81 m s^{-2}] and S is the average channel slope), and A represents a scour factor reflecting quasi-equilibrium bed conditions (see Engelund, 1974; Kikkawa et al., 1976; Zimmerman and Kennedy, 1978; Ikeda et al., 1981; Parker and Andrews, 1986; Ikeda, 1989; Odgaard, 1987; Chen and Duan, 2006) that can be estimated empirically following Pizzuto and Meckelnburg (1989). In our case, the scour factor equals 4.14 for the lower segment of the study reach and 2.52 for the upper segment (Table 1). Sun et al. (1996) approximated the derivative $\partial\alpha_i/\partial s$ in Equation 2 with the backward (upstream) difference $(\alpha_i - \alpha_{i-1})/\Delta s_i$.

Several workers (e.g., Howard and Knutson, 1984; Parker and Andrews, 1986; Odgaard, 1987; Furbish, 1988, 1991) have noted the tendency for freely migrating meanders to evolve into asymmetric planforms as their downstream limbs migrate more rapidly than their upstream limbs. Such a tendency is due to the effects of sustained curvature and the associated cross-stream bed topography that progressively advect high-momentum fluid outward, thereby increasing flow velocity along the length of the outer bank (Furbish, 1988, 1991). Because Equation 2 accounts for upstream curvature in the $\partial\alpha_i/\partial s$ term, the effects of sustained curvature are evident when the planforms of hypothetically shaped meanders evolve according to the solutions to Equation 1. We arbitrarily applied Equation 1 to hypothetically shaped meanders with channel characteristics similar to those of the lower segment of the study reach by assuming that ω_i was equal to zero at the reach entrance and then estimating this quantity at points downstream of the entrance using Equation 2.

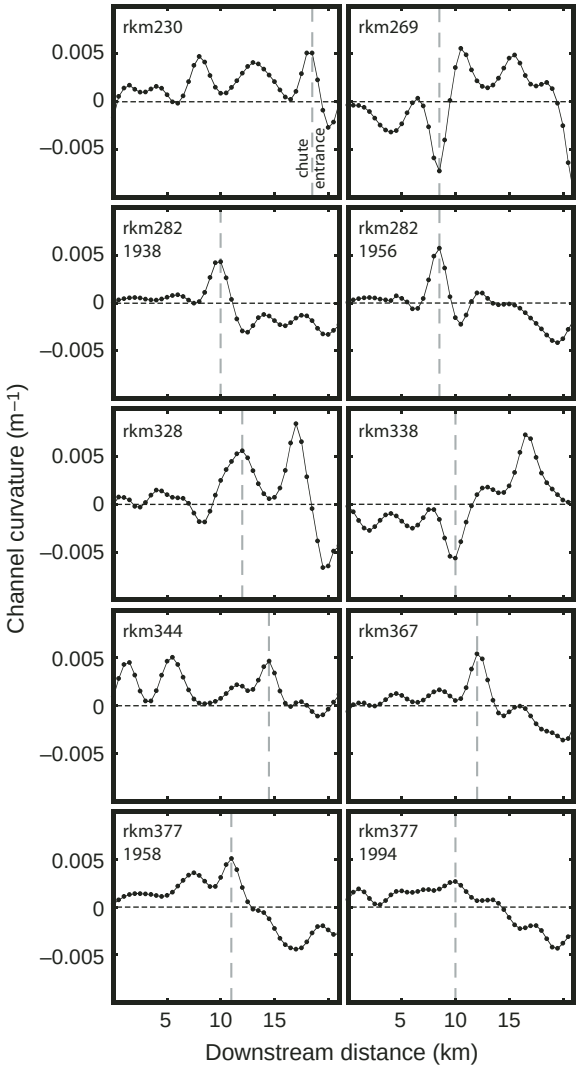

Figure 7. Curvature through the chute-producing historical reaches of the Sacramento River shown in Figure 5. The river kilometer (rkm) location of each reach is provided within the plot, as well as the year after incision took place for cases where cutoff occurred at the same location. The vertical, gray dashed lines illustrate the location of the chute entrance along the upstream meander. Inflections between meanders can be recognized when the sign of curvature changes, denoted wherever the data cross the horizontal, black dashed line.

Values used in solving the equations are shown in Table 1. If ε is spatially constant, the locus of peak curvature increases in magnitude and translates downstream as meanders evolve into ever more asymmetrical planforms, regardless of their initial shape (Fig. 8). This tendency to produce a locus of peak curvature within the downstream limb implies that, if all other variables are held constant, the evolution of the meander planform can produce conditions leading to embayment formation by localized riverbank incision. What remains to be determined, however, is the physical mechanism by which channel curvature exerts control on the location in the riverbank that is incised to form an embayment.

Characteristics of Overbank Flow through a Meandering Reach

To determine the ways in which channel curvature influences where overbank flows incise the floodplain, we examined characteristics of overbank flow through a segment of the study reach using the U.S. Geological Survey's Multi-Dimensional Surface Water Modeling System (MD-SWMS; Nelson et al., 2003). MD-SWMS provides an interface to several hydrodynamic models. The model used in this case was FaSTMECH, a hydrodynamic model that solves the vertically averaged, two-dimensional forms of the conservation of mass and momentum equations. Although the model does not account for all the effects of the three-dimensional nature of overbank flow through meandering reaches (see Nicholas and McLelland, 2004; Wormleaton et al., 2004), previous attempts to characterize overbank flow in flume experiments (e.g., Sellin et al., 1993; Shiono and Muto, 1998) and computer simulations (e.g., Bates et al., 2005) suggest that flow paths may be determined accurately using vertically averaged solutions. We therefore considered that the use of FaSTMECH would allow MD-SWMS to adequately represent flow conditions in a series of simple simulation experiments.

We conducted these experiments on a river segment within the study reach composed of two similarly shaped meander bends (Fig. 9), one of which began undergoing chute incision in 1974. The floodplain of the study segment is bounded by levees on either side, simplifying calculations of overbank flow. Topographic data for the segment were derived from a 1997 seamless channel and floodplain digital elevation model (DEM) composed of bathymetric data (0.6 m resolution) collected by the U.S. Army Corps of Engineers and interferometric synthetic aperture radar (INSAR) data (10 m resolution) of the floodplain. To simplify the simulations, topographic variations in the INSAR data caused by the presence of oxbow lakes and vegetation were removed. We conducted steady-flow simulations for four different discharges: one near bankfull discharge and the others at moderate flood discharges equivalent to 6 a, 60 a, and 120 a events during the post-1945 hydrologic regime (USGS gauge #11389000). We performed our simulation experiments using a regular grid mesh with one axis parallel to the valley centerline (Fig. 9). The resolution of the rectangular mesh was 30 m, roughly 15% of the bankfull channel width of the study segment and no more than 14% of the radius of curvature through the segment. The direct effects of the roughness of floodplain vegetation were momentarily ignored in the simulations, and we estimated roughness across the study segment using a nonuniform coefficient of drag based on flow depth.

Within the confined channel, the encounter of the downstream current with the outer bank helps adjust the course of river flow through the meander. The extent to which the outer bank must exert a force to adjust the flow's course is a function of channel curvature (Begin, 1981), indicated by the magnitude that the water surface is superelevated. In the case of overbank flow, the bank only weakly influences the free surface, and flow leaving the channel continues its path into the floodplain, as shown by the results of the MD-SWMS simulations (Fig. 10). At each of the simulated flood stages, the downstream component of depth-averaged flow velocity on the floodplain is highest at locations where the channel most strongly turns away from the downstream flow path, locations that occur at the actively incising chute and at three locations along the floodplain margin (denoted L1, L2, and L3 in Fig. 10). At these locations, flow is no longer steered by the riverbank but instead enters the floodplain, flowing at a direction that closely parallels the valley slope (the prevailing direction of which is represented by the centerline shown in Figs. 9 and 10). Results from flume studies

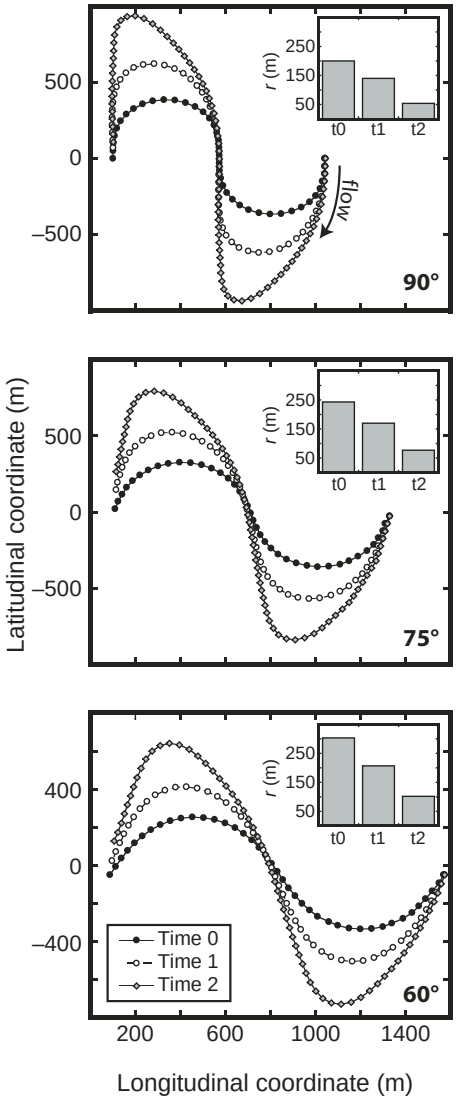

Figure 8. The evolution of hypothetically shaped meander centerlines with time. Each plot illustrates a uniquely shaped sinusoidal planform at time 0 (initial time step) with crossover angles of 90°, 75°, and 60°. Each centerline was discretized into 50 m spaced points, the locations of which were moved orthogonally to the centerline by distances equal to the migration rate as solved using Equation 1 in the text. Migration rates, based on solutions to Equation 2 using values of the lower segment of the Sacramento River (Table 1), were determined during bankfull conditions. At each time step, the new centerline was discretized and curvature was recalculated using a method described in the text. The inset within each plot illustrates the magnitude of the minimum radius of curvature (*r*), the inverse of which is local curvature, with each time step. In each case, flow is from right to left.

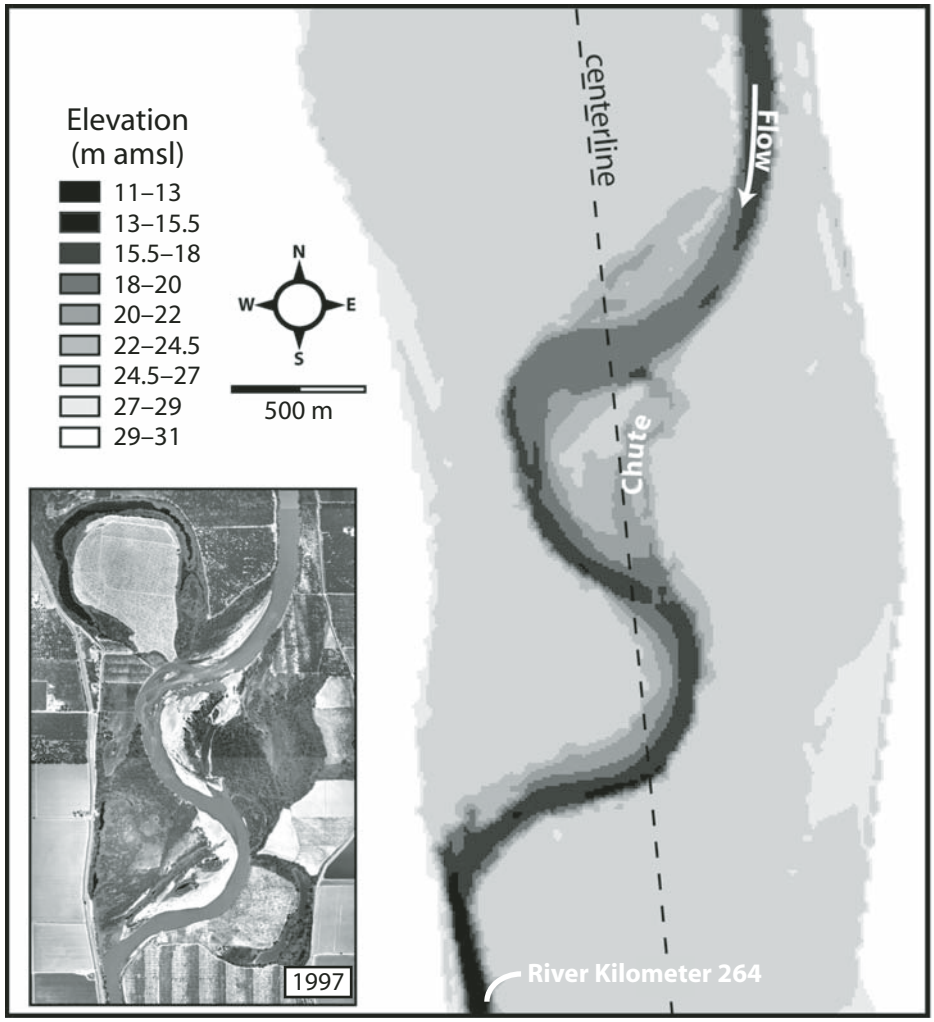

Figure 9. Input topography for the segment of the study reach used in the MD-SWMS simulations. Elevation is provided in units of meters above mean sea level (m amsl). An aerial photo of the segment in 1997 is provided as an inset. Topographic variations due to oxbow lakes and vegetation (both of which can be seen in the photo) were removed from the topographic input data, resulting in a planar floodplain with a chute (labeled). The valley centerline used in building the grid mesh for the MD-SWMS simulations is shown as the black dashed line.

support the MD-SWMS prediction that water is rapidly expelled from the meandering channel onto the floodplain where the channel turns away from the downstream flow path (Sellin et al., 1993; Knight and Shiono, 1996; Shiono and Muto, 1998; Wormleaton et al., 2004), which then increases boundary shear stress along the floodplain margin (Sellin and Willetts, 1996). MD-SWMS also predicts zones of high boundary shear stress at L1, L2, and L3, as well as in the actively incising chute (Fig. 11). Boundary shear stress on the floodplain remains fairly constant above a discharge of 4000 $m^3 s^{-1}$, with magnitudes locally approaching those within the channel at a discharge of 1500 $m^3 s^{-1}$. The fact that shear stress remains fairly constant over varying flood discharges is due to the model prediction that the flood's water surface becomes less steep as discharge increases, a prediction based on the way drag was estimated for the floodplain. Field measurements of the flood's water surface during several flood discharges would make the estimate of drag in future work more precise. Nonetheless, the predicted magnitudes of boundary shear stress in this study imply that, in the absence of vegetation, the sandy-silty floodplain surface, with an estimated critical shear stress of ~0.1 Pa (based on a Shields calculation using a median grain size of 0.13 mm and a Shields number of 0.045), should be most susceptible to erosion at

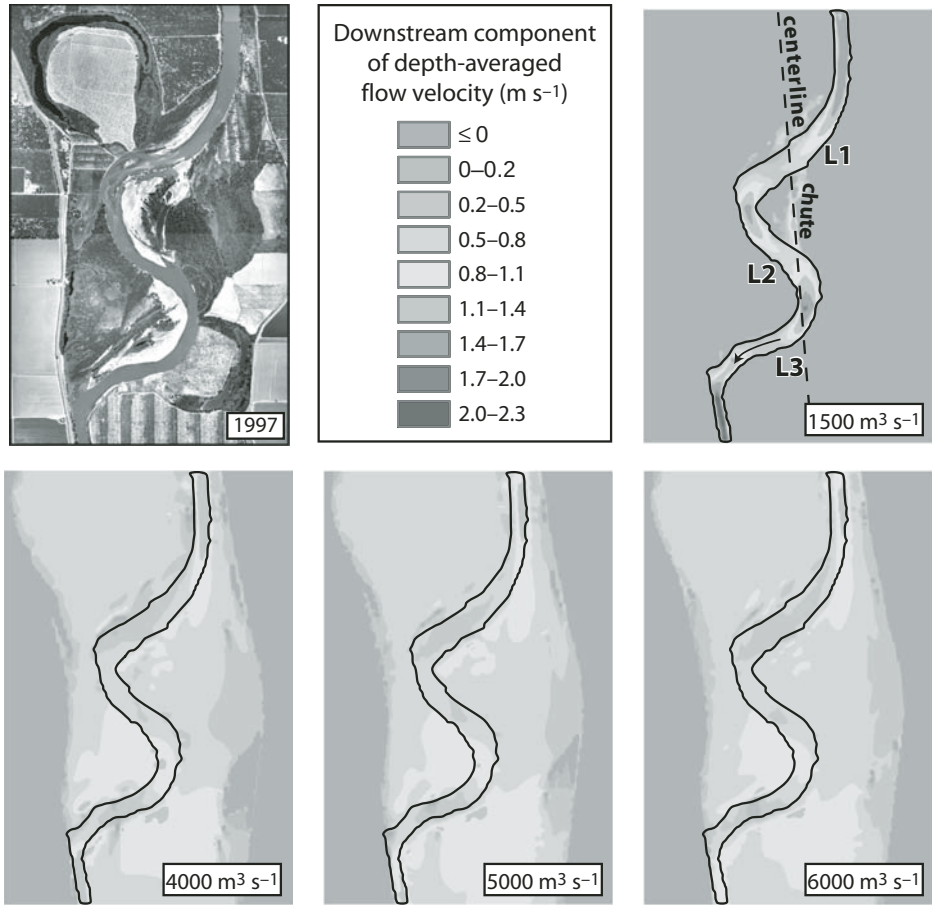

Figure 10. Results from MD-SWMS simulations showing magnitudes of the downstream component of the depth-averaged flow velocity for four different, steady discharges. The downstream component is parallel to the dashed centerline (shown in the upper right map) from which the grid mesh was constructed. All discharges, except for 1500 $m^3 s^{-1}$, represent overbank flows. An aerial photo is provided of the simulated segment of the study reach, located upstream of river kilometer 264. A black outline of the 1500 $m^3 s^{-1}$ channel has been drawn into each map. Flow velocities are generally highest on the floodplain at locations L1, L2, and L3 shown in the upper left map. A color version of this figure is available in the GSA Data Repository.[1]

L1, L2, L3, and the chute. Boundary shear stress gradually declines in the downstream direction within the chute as overbank flow leaving the main channel loses momentum via mixing with low-momentum fluid.

The fact that the chute has not evolved to cut off the entire channel discharge in over 30 a may be due to the influx of sediment from the main channel that fills in, or partly heals, the depression during smaller flood events that are not capable of transporting all the sediment delivered to the floodplain out of the floodplain and back into the river (Slingerland and Smith, 1998). Complete healing of the chute may be prevented because the lack of vegetation at this location has localized floodplain erosion during larger flood events that are capable of transporting all the sediment delivered to the floodplain as well as sediment eroded from the floodplain surface. Given our observations that embayments are incised only where the floodplain is bare or lightly vegetated, the natural or artificial removal of floodplain vegetation where the channel most strongly turns away from the downstream flow path appears to increase the susceptibility of the floodplain to incision. In the following section, we quantify the degree to which floodplain vegetation must be thinned before chute incision by embayment formation and extension takes place.

[1]GSA Data Repository item 2009210, Color versions of figures 10 and 11, is available at http://www.geosociety.org/pubs/ft2009.htm or by request to editing@geosociety.org.

PHYSICAL CONDITIONS FOR EMBAYMENT FORMATION

Development of a One-Dimensional Flow Model

Where channel curvature is greatest, more of the downstream current impinges directly upon the outer bank, driving an outer-bank cell of circulating fluid that flows opposite to that of the secondary current (Markham and Thorne, 1992). The importance of curvature on the forces exerted by flow impinging upon the outer bank was previously theorized by Begin (1981), and the outer-bank cell has been independently observed in natural settings (Bathurst, 1979; Thorne and Hey, 1979; Thorne et al., 1985). Markham and Thorne (1992) speculated that the cell of circulating fluid was capable of localizing bank erosion, leading to the formation of an embayment within the floodplain margin. Localized bank erosion by this mechanism may explain the embayments we observed along the Sacramento and Missouri Rivers, but embayment formation by an outer-bank cell of circulating fluid requires verification. Even so, field observations (Hooke, 1995; Gay et al., 1998; Fuller et al., 2003) make clear that floods are required for the formation of a chute, and so the influence of an embayment on floodplain incision may result from its existence as a topographic depression within the bank that provides a floodplain conduit for overbank flows. As a consequence, an embayment could generate positive feedback as more flow is focused into the depression, leading to increased incision and the extension of the embayment into the floodplain, a scenario also recognized by Markham and Thorne (1992).

If embayments are precursors to chute incision in large rivers with uniform floodplain topography, then an understanding of what controls their formation could clarify where chute cutoffs are likely to occur. Because bank erosion by an outer-bank cell of circulating fluid has not been directly observed, we sought to identify conditions that would allow overbank flows alone to form an embayment by incising the riverbank. The erosive ability of overbank flows is determined by the boundary shear stress exerted onto the floodplain, which is a function of flood hydraulics and floodplain roughness in the form of vegetation and topographic variability. We constructed a model of overbank flow through a vegetated floodplain and simplified our analysis by considering the floodplain as a planar surface with a slope equal to the mean valley gradient. Our analytical framework consisted of two control volumes (Fig. 12) encompassing: (1) the flow entering the floodplain, and

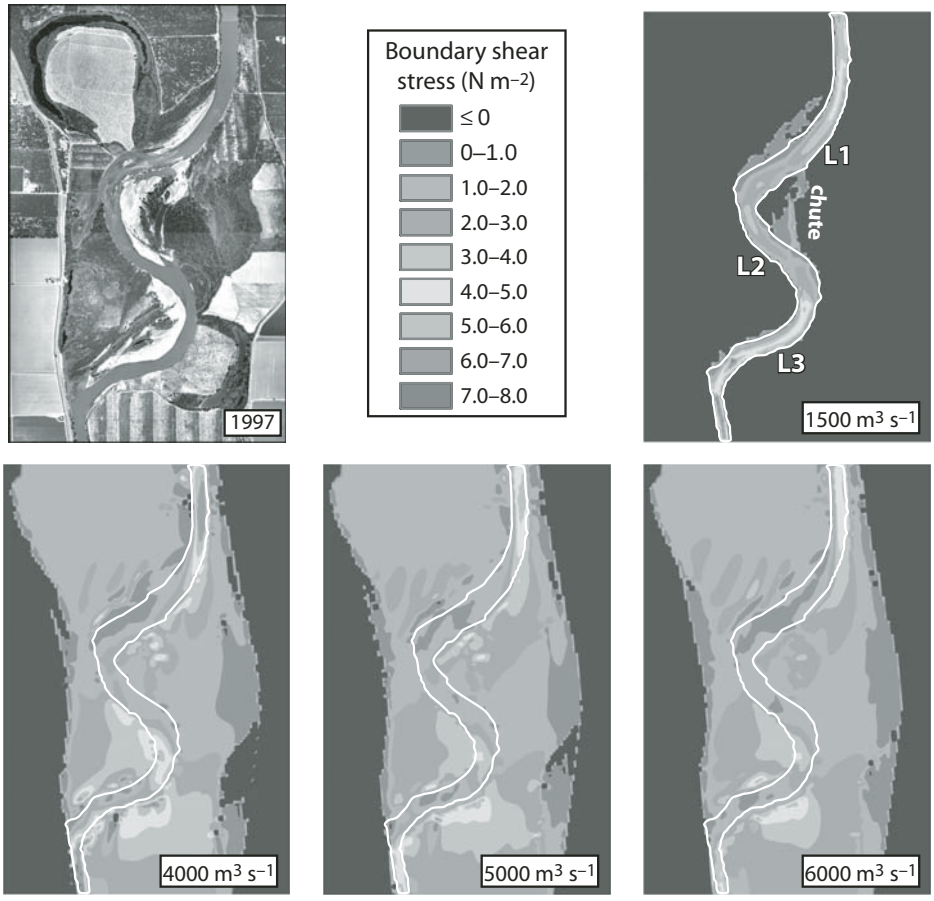

Figure 11. Results from MD-SWMS simulations showing magnitudes of boundary shear stress for four different, steady discharges. All discharges, except for 1500 $m^3 s^{-1}$, represent overbank flows. An aerial photo is provided of the simulated segment of the study reach, located upstream of river kilometer 264. A white outline of the 1500 $m^3 s^{-1}$ channel has been drawn into each map. Maximum zones of boundary shear stress on the floodplain generally occur where the channel curvature is greatest, or where the channel most greatly turns from the downstream flow path (labeled L1, L2, and L3 in the upper left map), and within the chute. A color version of this figure is available in the GSA Data Repository (see footnote 1).

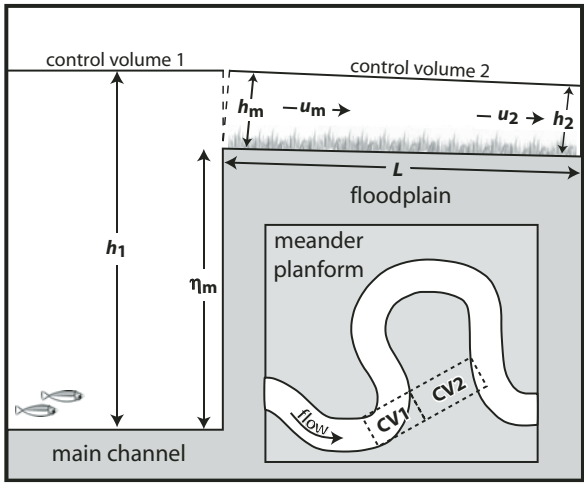

Figure 12. Schematic illustrating the control-volume perspective from which our model of overbank flow was developed. Flow within the main channel has a depth equal to h_1 and enters the floodplain from control volume 1 (CV1) to control volume 2 (CV2). Flow in the floodplain (CV2) has an initial depth-averaged velocity of u_m and depth of h_m. Flow returning from the floodplain into the main channel has a depth-averaged velocity of u_2 and a depth of h_2. The height of the channel bank is represented by η_m.

(2) the flow over the floodplain. The relevant flow parameters can then be predicted if conservation of mass and momentum is applied to the flows within the control volumes. In Figure 12, CV1 represents the flow transition from the main channel to the floodplain, whereas CV2 treats the flow over the floodplain. Due to the complexity of the transition region in CV1, conservation of mass and momentum cannot be fully satisfied in the analysis because an unknown portion of the flow proceeds down the main river channel while the remaining portion escapes onto the floodplain. The precise nature of the flow in this region will determine how an embayment is carved out of the bank, but predicting details of this would require a full three-dimensional flow model. However, a set of reasonable assumptions about the nature of the flow in CV1 coupled with the physics of CV2 suggests that the flow over the floodplain dominates overbank flows. We can therefore learn much about chute formation by looking exclusively at the floodplain control volume CV2, an approach similar to that of Slingerland and Smith (1998) and Smith (2004).

In our analytical approach, we neglect the role of vegetation in generating turbulence within the overbank flow (e.g., wake in the lee side of a submerged plant) and consider that the total drag exerted by the flow varies linearly with the number of submerged plants on the floodplain, a consideration supported by the results from both experimental and theoretical work (Nepf, 1999; Luhar et al., 2008). We ignore the effects of densely spaced vegetation on the shape of the flood velocity profile (see White and Nepf, 2008) but acknowledge that we may thus overestimate predictions of boundary shear stress on the vegetated floodplain. Given these conditions, if we assume that the floodplain flow within CV2 is of approximately constant width, conservation of mass yields:

$$u_m h_m = u_2 h_2, \tag{3}$$

where u_m and u_2 represent the depth-averaged flow velocities, and h_m and h_2 represent the flow depths at the inlet and outlet of CV2. From conservation of momentum:

$$\frac{\rho g h_m^2}{2} - \frac{\rho g h_2^2}{2} + \frac{\rho g (h_m + h_2)}{2} L \sin\beta = -\rho u_m^2 h_m + \rho u_2^2 h_2 + \tau_{fp} L, \tag{4}$$

where ρ represents fluid density (1000 kg m^{-3}), β represents the inclination angle of the floodplain in the down-valley direction, L represents the length of the floodplain over which chute incision takes place, and τ_{fp} represents the average

total shear stress exerted by the overbank flow, including both the boundary shear stress and the stress exerted on vegetation. Smith (2004) considered that the drag associated with submerged vegetation extracts momentum from the overbank flow that otherwise would be available for sediment transport and erosion. Given this, Smith (2004) stated that the total shear stress exerted by the flow through a vegetated floodplain would be:

$$\tau_{fp} = (1+\sigma_D)\tau_{0,m}, \quad (5)$$

where $\tau_{0,m}$ represents the boundary shear stress on the underlying surface at the floodplain margin, and σ_D represents a drag term given by:

$$\sigma_D = \xi \frac{C_D}{2\kappa^2}\left[\ln\left(\frac{h}{z_0}\right) - 0.74\right]^2. \quad (6)$$

Here, C_D represents the drag coefficient for a stem or branch, κ is von Karman's constant, h represents flow depth, z_0 represents a roughness parameter for the floodplain surface, and ξ represents a nondimensional parameter that accounts for the area of the bed affected by submerged vegetation, given by:

$$\xi = \frac{h_v \delta}{a^2}, \quad (7)$$

where δ represents the diameter of stems or branches, h_v represents the submerged extent of vegetation (assumed to be the water depth if vegetation extends throughout the water column), and a represents the average distance between stems or branches. We specified z_0 as $d_{50}/30$, and the median grain size was set to 0.13 mm based on the estimate of surficial bank sediment as reported earlier. Floods of the Sacramento River last for days (Singer and Dunne, 2004b), and during the approximately steady near-peak portion of the flood hydrograph, the boundary shear stress, as suggested by Smith (2004), is

$$\tau_{0,m} = \frac{1}{8}\rho f\left[\frac{(u_m + u_2)}{2}\right]^2, \quad (8)$$

where f represents the Darcy-Weisbach friction factor, which was set equal to 0.017 for the fine-grained floodplain.

Solutions to this system of equations allowed us to estimate the boundary shear stress exerted by overbank flow as a function of flood characteristics and the structure of floodplain vegetation. We simplified our analysis by assuming that plants were uniformly distributed across the floodplain surface and were of similar size. We then examined drag effects within two different floodplain environments: a floodplain vegetated only by grasses and another vegetated only by woody vegetation. For the grassy floodplain scenario, C_D was set to a constant value of 0.05 based on flume experiments planted with real grass (Wilson and Horritt, 2002). For the wooded floodplain, each plant was represented as a vertical cylinder, and C_D was set to 1.2 after Kean and Smith (2005). By ignoring the additional roughness presented by leaves and branches, we were able to quantify the minimum spacing on the floodplain between similarly sized stems that would protect the floodplain from incision, a variable denoted as a_{crit}. If the presence of leaves and branches could be successfully generalized and quantified in future work, their likely effect would be to increase the spacing of vegetation needed to reduce the stress applied to the floodplain by overbank flow.

Quantifying the Effects of Submerged Floodplain Vegetation

In describing the effects of floodplain vegetation on overbank flow, we first solved Equations 3–8 for the inlet and outlet velocities of CV2 by assuming that the inlet and outlet depths were the same ($h_m = h_2$). The solutions that result are generally consistent with field observations and intuitive understanding. Given a floodplain vegetated by uniformly spaced woody plants with a constant stem diameter of 0.5 cm, the model predicts that the boundary shear stress exerted by the overbank flow across the floodplain margin increases as the plants are more widely spaced (Fig. 13A). Boundary shear stress generally declines with increases in flood depth because more of the plants become submerged, increasing the frontal area of roughness elements. As a result, the flow continues to slow as it enters the floodplain, lowering the boundary shear stress despite the fact that flow depths are increasing. The exception occurs when plants are so widely spaced ($a/\delta \geq 1000$) that effectively no drag is being exerted on the vegetation by the overall flow, resulting in increased boundary shear stress with increases in flood depth. The model also predicts that in nearly all circumstances, overbank flow slows upon entering the floodplain as stage rises above bankfull (Fig. 13B). Except when plants are widely spaced ($a/\delta \geq 1000$), overbank flow continues to slow upon entering the floodplain with increases

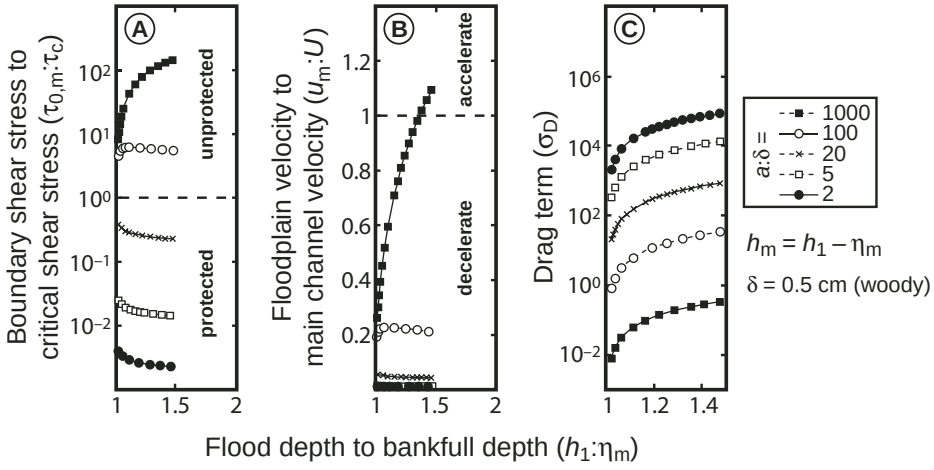

Figure 13. (A) The ratio of boundary shear stress to critical shear stress across the floodplain margin as determined using solutions to Equations 3–8 in the text plotted against the ratio of flood depth over the main channel to bankfull depth (h_1:η_m). Solutions show that the ratio increases as the spacing between plants (a) increases for a constant stem diameter (δ) of 0.5 cm on a floodplain with a median grain size of 0.13 mm for surficial sediment. The critical shear stress value used here is based on field experiments reported in Constantine (2006) and equals 0.1 N m^{-2}. (B) The ratio of the depth-averaged flow velocity over the floodplain margin to the cross-sectionally averaged flow velocity in the main channel plotted against h_1:η_m. Cross-sectionally averaged flow velocities in the main channel were obtained from HEC-RAS simulations using cross sections within the lower segment obtained from bathymetry collected by the U.S. Army Corps of Engineers. Simulations were conducted over a range of flood stages. (C) A drag term determined using Equation 6 in the text plotted against h_1:η_m. The depth of flow over the floodplain margin (h_m) is equal to the difference between h_1 and η_m.

in stage because plants become increasingly submerged. In the case of $a/\delta = 1000$, flow velocities across the floodplain increase with increases in flood depth, and overbank flow entering the floodplain is predicted to accelerate as flood stage rises above ~1.5 times the bankfull depth due to the floodplain sloping more steeply than the channel; because of the condition specifying $h_m = h_2$, the flow does not continue to accelerate over the floodplain. As expected, the model also predicts that the drag term σ_D increases as vegetation becomes more closely spaced because the flood is forced to flow through a greater density of plants (Fig. 13C).

The assumption that h_m equals h_2 allowed us to make a simple calculation of the critical spacing distance (a_{crit}) between uniformly spaced plants of similar stem diameter above which the floodplain is no longer protected from incision (or when the boundary shear stress equals the critical shear stress required to mobilize floodplain sediment) (Fig. 14). We found that this critical spacing distance for woody plants increases as the depth of submergence increases. The same is true for grass until the flood overtops the plants, after which a_{crit} declines with increasing flood stage. The model also predicts that large trees can be spaced farther apart on the floodplain than small woody plants while protecting the floodplain from incision. As flood stage rises up to ~1.5 times the bankfull depth, a_{crit} ranges from 1.5 to 1.6 m when δ equals 32 cm, in contrast to a_{crit} ranging from 0.17 to 0.22 m when δ equals only 0.5 cm. Although a_{crit} declines with δ because a larger stem presents a larger frontal area that the overbank flow must overcome, there is a limit to how closely large trees can be spaced given that their crowns do not generally intersect. For example, cottonwood (*Populus fremontii*) is the common riparian tree during the early succession of the Sacramento River's riparian forest, and it has mature trunk diameters >32 cm (Sedgwick and Knopf, 1986; Rowland et al., 2000) and crown diameters between 10 and 30 m (Farid et al., 2006). Given a δ value of 32 cm, the closest that cottonwood trees can be spaced is roughly between 31 and 94 stem diameters, greater than the a_{crit}/δ value predicted by the model for this stem size (Fig. 14). The spacing between the branches of small woody plants and brush is not limited by large crown diameters, and the number of low-lying stems and branches of this kind of vegetation can greatly reduce *a*. As a result, the model predicts that for any flood stage, small woody plants can be spaced much farther apart relative to their stem diameters than large trees while protecting the floodplain from incision. This finding is the same as that of Smith (2004), and it suggests that a floodplain vegetated by small woody plants or brush is less likely to undergo chute cutoff than one vegetated solely by large trees.

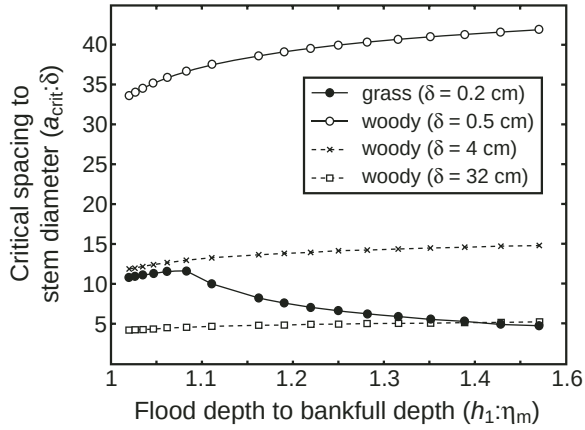

Figure 14. The ratio of the critical spacing distance between floodplain plants to stem diameter plotted against the ratio of flood depth to bankfull depth. The critical spacing distance represents the distance above which floodplain erosion could occur. Curves for grass and woody plants of varying stem diameters (δ) are plotted. Woody plants were considered tall enough to remain submerged throughout all flood stages. Grass plants were modeled using a constant height of 0.5 m.

Although solutions to Equations 3–8 are dependent on our assumptions, our conclusions are fairly insensitive to the choice of inputs. The assumption that generates the greatest variation in the results is $h_m = h_2$. If we assume that $h_2 = h_1 - \eta_m$, where h_1 represents the average channel depth and η_m represents the bankfull channel depth, h_m can instead be stated as:

$$h_m = h_2 + c\frac{WU^2}{2gr}, \quad (9)$$

where *c* represents a coefficient used to modulate the degree to which the water surface is superelevated by centrifugal forcing, and *W* represents the bankfull channel width. The centrifugal force term $WU^2/2gr$ in Equation 9 is an estimate of the magnitude of superelevation during fully developed flow based on a cross-stream force balance that does not consider the effects of internal friction caused by the vertical diffusion of cross-stream momentum. The centrifugal force that superelevates the cross-stream water surface is likely dampened during flood conditions, and thus *c* was used to lower the estimate of superelevation, where $0 \le c \le 1$. The equation also presumes that, at the outlet, overbank flow reenters the river at a point where the water surface is not superelevated. Solving Equations 3–8 using Equation 9, we found that our original conclusions about the importance of small woody vegetation remained unchanged (Fig. 15). As *c* increases, the greater free surface slope over the floodplain results in greater boundary shear stress, and hence a smaller critical separation distance. Nevertheless, the smaller woody vegetation remains, the more

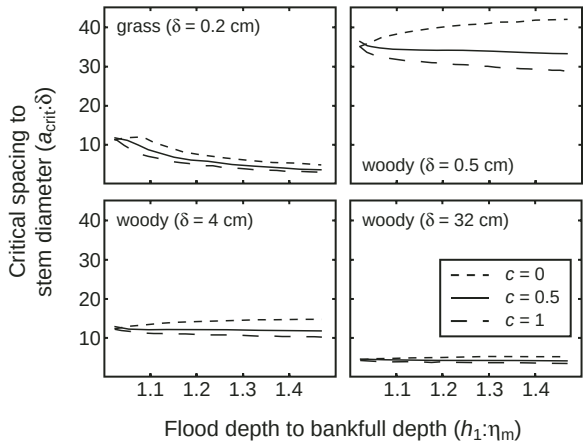

Figure 15. The ratio of the critical spacing distance between floodplain plants to stem diameter plotted against the ratio of flood depth to bankfull depth based on solutions to the Equations 3–9 in the text. Curves are based on the degree that the water surface is superelevated, a function of the coefficient *c* in Equation 9. Solutions are provided for grass and woody plants of varying stem diameters (δ). Woody plants were considered tall enough to remain submerged throughout all flood stages. Grass plants were modeled using a constant height of 0.5 m.

effective it is at protecting the floodplain from erosion.

Although the model predicts that a floodplain vegetated solely by large trees may be less capable of protecting the floodplain from incision than one vegetated by small woody plants or brush, the role of large trees during the ecological succession of the floodplain may be important in preventing chute cutoff. During the early succession of the Sacramento River's riparian forest, shade-tolerant brush plants fill up the understory of the cottonwood canopy (Buer, 1994), thus lowering *a* to values much less than 1 m and providing nearly a 100% plant cover (Harris, 1987). As the riparian forest matures, valley oak (*Quercus lobata*), with mature diameters >80 cm (Griggs and Golet, 2002), becomes the dominant riparian tree. During this stage, the understory clears, and plant cover is reduced by at least 30% (Harris, 1987), perhaps making the maturing riparian forest more susceptible to floodplain erosion. Even so, in environments where shade-tolerant brush and woody plants require a canopy to allow them to out-compete fast-growing, shade-intolerant grasses, the presence of large trees on a natural floodplain will likely reduce the occurrence of chute cutoff, especially when contrasted to riverbanks lightly vegetated by grasses or orchards in which the understory is artificially cleared.

Figure 16. The ratio of the critical spacing distance between floodplain plants to stem diameter plotted against the ratio of flood depth to bankfull depth based on solutions to the Equations 3–9 in the text. Curves are based on different values of floodplain slope (sin β). Solutions are provided for grass and woody plants of varying stem diameters (δ). Woody plants were considered tall enough to remain submerged throughout all flood stages. Grass plants were modeled using a constant height of 0.5 m.

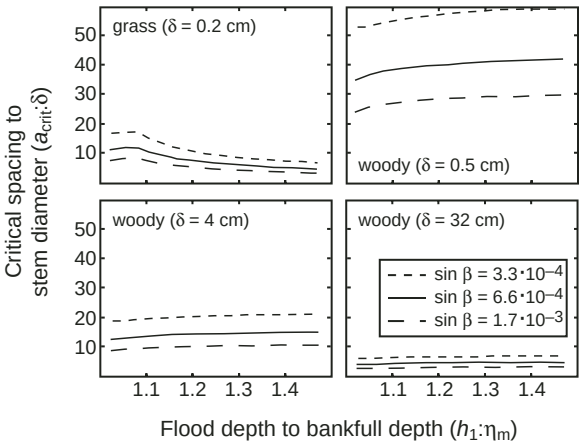

Implications for the Evolution of Large Meandering Rivers and their Floodplains

From the various empirical and theoretical observations made thus far, it is possible to recognize at least three primary controls on the occurrence of chute cutoff by embayment formation and extension. Whether a flood will incise the riverbank to form an embayment will depend upon whether overbank flow creates sufficient boundary shear stress to entrain floodplain sediment and whether it has sufficient momentum to transport the eroded sediment, as well as any sediment delivered from the main channel, out of the floodplain. The first control, then, on the occurrence of chute cutoff is valley slope (sin β in Eq. 4), which propels the flow across the floodplain. Our model of flow through a vegetated floodplain predicts that vegetation must be spaced more closely together as floodplain slope increases in order to protect the floodplain from incision, regardless of the type or size of floodplain vegetation (Fig. 16). As a consequence, chute cutoff will be more common along rivers flowing through steep valleys, other factors being constant.

If embayment formation is the dominant mechanism of chute cutoff along large meandering rivers with uniform floodplain topography, then the characteristics of floodplain vegetation will greatly influence the planform evolution of such rivers, making the structure of floodplain vegetation the second control on the occurrence of chute cutoff. When floodplain vegetation is so dense that chute cutoff cannot occur, neck cutoff is the only process of channel shortening, allowing the meandering river to evolve into a highly sinuous planform (Howard and Knutson, 1984; Howard, 1996; Sun et al., 1996; Stølum, 1998; Camporeale et al., 2005). When floodplain vegetation is sufficiently thinned, naturally or artificially, for chute cutoff to occur, sinuosity is reduced as meanders become shortened by the increased rate of production of oxbow lakes (Constantine and Dunne, 2008). Hence, floodplain vegetation and valley slope explain differences in planform (i.e., sinuosity, meander amplitude) and floodplain (i.e., topographic variability, meander-belt width) characteristics among rivers such as the Wood River (valley slope of 0.0018–0.0025, sinuosity of 1.9–2.1) and the Teklanika River (valley slope of 0.0018–0.0019, sinuosity of 2.1–2.9), in Alaska (D.J. Furbish, 2008, personal commun.), and the Sacramento River (valley slope of ~5×10^{-4}, sinuosity of 1.4) in California, and the Purus River of Brazil (valley slope of ~6×10^{-5}, sinuosity of 2.3).

Several workers have documented the importance of floodplain vegetation on fluvial geomorphology. In addition to the considerable research describing the effects of riparian forest on meander migration (e.g., Pizzuto and Meckelnburg, 1989; Simon and Collison, 2002; Perucca et al., 2007), field (e.g., Mackin, 1956, Wood River, Idaho, USA; Millar, 2000, Slesse Creek, British Columbia, Canada), laboratory (e.g., Gran and Paola, 2001; Tal and Paola, 2007), and numerical (e.g., Murray and Paola, 2003) observations suggest that floodplain vegetation is required to prevent the meandering river from transitioning into a braided river. From flume experiments, Ashmore (1991) observed that the transition from a meandering to a braided channel took place via multiple occurrences of chute cutoff, and so the structure of floodplain vegetation may not only influence rates of meander migration, but it may also affect the process that Smith (2004) termed floodplain unraveling, or the condition in which the floodplain surface is highly mobile. Depending on the density of floodplain vegetation, the rate of floodplain unraveling can lead either to infrequent occurrences of chute cutoff or to such frequent occurrences of the process that the meandering river is at risk of becoming multithreaded, even while sediment loading is constant. Because environmental controls on the structure of floodplain vegetation are dependent on geographic setting (i.e., as determined by climate and tectonics) (Hupp and Osterkamp, 1996), the frequency of chute cutoff along any meandering river is a function of environmental context, and so differences in the geomorphological characteristics of meandering rivers and their floodplains should be expected to vary systematically with geography.

As a river's suspended load increases, more sediment should be delivered to the floodplain, potentially balancing any erosion if not promoting aggradation. Some evidence suggests that occurrences of meander cutoff along the Sacramento River may be correlated with spatial trends in suspended sediment discharge, and so it seems that a third control on the occurrence of chute cutoff is the nature and quantity of sediment in transport during a flood. Benninger et al. (2002) mapped historical occurrences of cutoff along the Sacramento River using a 93 a record of historical maps and aerial photos and found that the frequency of cutoff was highest along

a segment of the river that Singer and Dunne (2001) determined to carry small volumes of suspended sediment. Between 1904 and 1997, a segment of the Sacramento River in which the historically averaged suspended sediment discharge was 1–3 Mt a^{-1} experienced cutoff roughly once every kilometer of river. During the same time span, another segment of the river in which historically averaged suspended sediment discharge was ~7 Mt a^{-1} experienced cutoff only once every 2.5 km of river.

Several studies have reported that in the absence of environmental changes, the curvature characteristics of a meandering river should remain fairly stable through time as meander growth becomes balanced by meander cutoff in the long term (Howard and Knutson, 1984; Hooke and Redmond, 1992; Stølum, 1996; Camporeale et al., 2005). Our results help define the kinds of environmental change (e.g., steepening of valley slope, thinning of floodplain vegetation, reduction of sediment load) that would offset the balance between meander growth and cutoff, thereby directly affecting channel sinuosity and rates of meander migration. Because physical changes in valley slope occur more slowly than do changes in floodplain vegetation or sediment loading, the latter two controls on the occurrence of chute cutoff by embayment formation and extension are most important in determining the response of meandering rivers to environmental change, whether climate driven or directly anthropogenic. Future efforts to improve theoretical understanding of meandering dynamics in the context of changing environmental conditions should aim to explicitly incorporate the effects of changes in the structure of floodplain vegetation as well as in the nature and quantity of sediment in transport.

CONCLUSIONS

Three different mechanisms of chute cutoff along meandering rivers were identified in the field. Depending on the environmental context, chute cutoff may happen by the enlargement of swales, headcut extension during locally induced flooding, and by the downstream extension of an embayment during a sequence of floods. Along large meandering rivers with uniform floodplain topography, such as the Sacramento River in California, USA, the formation of embayments is observed to be the initiating mechanism of chute cutoff. Along the Sacramento River, embayments tend to form where channel curvature is greatest just upstream of the inflection of the meander that undergoes cutoff. Our hydrodynamic modeling suggests that this tendency is due to overbank flow escaping from the main channel where riverbanks most strongly turn away from the downstream flow path, locations along the river where the water surface is most superelevated. At these locations, river flow sustains its direction into the floodplain, creating a zone of high boundary shear stress on the channel-floodplain margin. The ability of rivers to incise their banks depends on the structure of floodplain vegetation, illustrated by the fact that chutes along the Sacramento River formed only within bare or sparsely vegetated portions of the floodplain. A simple one-dimensional model of flow through riparian vegetation indicates that a floodplain vegetated by small woody plants or brush is most resistant to chute incision. Although large trees alone may not sufficiently prevent incision, their presence may influence the occurrence of chute cutoff by fostering the growth of small, shade-tolerant woody plants. Our findings suggest that chute cutoff by embayment formation and extension is most likely along large meandering rivers having steeply sloping floodplains and vegetation that naturally lacks a dense understory or consists solely of grasses, as well as those having floodplains altered by land use.

APPENDIX. NOTATION

- α Local curvature
- a Vegetation spacing
- a_{crit} Critical vegetation spacing above which floodplain erosion can occur
- A Scour factor
- b Average bankfull half-width or $W/2$
- β Inclination angle of the floodplain in the downvalley direction
- C_D Drag coefficient
- C_f Dimensionless friction coefficient
- δ Stem diameter
- d_{50} Median particle diameter
- d_{84} 84th percentile particle diameter
- ε Dimensionless coefficient of erodibility
- E Outer-bank erosion rate
- f Darcy-Weisbach friction factor
- g Gravitational acceleration
- h_1 Flow depth within the center of the main channel
- h_m Overbank flow depth on floodplain margin
- h_2 Overbank flow depth on at floodplain outlet
- h_v Submerged extent of floodplain vegetation
- I Channel centerline location
- η_m Bankfull channel depth
- κ von Karman's constant
- L Length of floodplain over which chute incision occurs
- R Local radius of curvature or $1/\alpha$
- ρ Fluid density
- σ_D Dimensionless coefficient reflecting drag effects on shear stress
- Δs Change in distance between centerline points
- S Average downstream channel slope
- τ_{fp} Average total stress on floodplain
- $\tau_{0,m}$ Boundary shear stress on floodplain margin
- U Bankfull, reach-averaged downstream flow velocity within channel
- u_m Downstream flow velocity over floodplain margin
- u_2 Downstream flow velocity exiting the floodplain
- ω Near-bank velocity term
- W Average bankfull channel width
- ξ Dimensionless parameter reflecting area of bed affected by submerged vegetation
- y Average bankfull channel depth
- ζ Superelevation of water surface
- z_0 Roughness parameter

ACKNOWLEDGMENTS

The authors thank Jon Major, David Jon Furbish, Jonathan Nelson, and an anonymous reviewer for critiques that significantly improved the paper. The authors are also grateful to Paul Bates, Douglas Burbank, Edward Keller, Candice Constantine, and Carl Legleiter for helpful conversations that improved the study. Aerial photos of the Sacramento River were provided by the California Department of Water Resources. Technical assistance was provided by Allison Groom, Candice Constantine, Michael Singer, and Carl Legleiter. A Eugene-Cota Robles Fellowship of the University of California provided student support for Constantine. The research was supported by CALFED grant 4600002659 and the Don J. Easterbrook Award of the Geological Society of America.

REFERENCES CITED

Aalto, R., Lauer, J.W., and Dietrich, W.E., 2008, Spatial and temporal dynamics of sediment accumulation and exchange along Strickland River floodplains (Papua New Guinea) over decadal-to-centennial timescales: Journal of Geophysical Research, v. 113, p. F01S04, doi: 10.1029/2006JF000627.

Alonso, C.V., Bennett, S.J., and Stein, O.R., 2002, Predicting head cut erosion and migration in concentrated flows typical of upland areas: Water Resources Research, v. 38, no. WR001173, doi: 10.1029/2001WR001173.

Ashmore, P.E., 1991, How do gravel-bed rivers braid?: Canadian Journal of Earth Sciences, v. 28, p. 326–341.

Bates, P.D., Horritt, M.S., Hunter, N.M., Mason, D., and Cobby, D., 2005, Numerical modelling of floodplain flow, *in* Bates, P.D., Lane, S.N., and Ferguson, R.I., eds., Computational Fluid Dynamics: Applications in Environmental Hydraulics: New York, John Wiley & Sons, p. 271–304.

Bathurst, J.C., 1979, Distribution of boundary shear stress in rivers, *in* Rhodes, D.D., and Williams, G.P., eds., Adjustment of the Fluvial System: Proceedings of the 10th Annual Geomorphology Symposium: New York, HarperCollins, p. 95–106.

Begin, Z.B., 1981, Stream curvature and bank erosion: A model based on the momentum equation: The Journal of Geology, v. 89, p. 497–504.

Benninger, L.M., Micheli, E.R., and Larsen, E.W., 2002, Historic channel cut-off on the Sacramento River, California, USA: International Symposium on the Structure, Function and Management Implications of Fluvial Sedimentary Systems [abs.]: Alice Springs, Australia, International Association of Hydrological Sciences, p. 4–7.

Bridge, J.S., Smith, N.D., Trent, F., Gabel, S.L., and Bernstein, P., 1986, Sedimentology and morphology of a low-sinuosity river: Calamus River, Nebraska Sand Hills: Sedimentology, v. 33, p. 851–870, doi: 10.1111/j.1365-3091.1986.tb00987.x.

Brush, L.M., and Wolman, M.G., 1960, Knickpoint behavior in noncohesive material: A laboratory study: Geological Society of America Bulletin, v. 71, p. 59–74, doi: 10.1130/0016-7606(1960)71[59:KBINMA]2.0.CO;2.

Buer, K., 1994, Sacramento River Bank Erosion Investigation Memorandum Progress Report: Red Bluff, California Department of Water Resources, Northern District, 126 p.

California Department of Water Resources, 1979, Observations of Sacramento River Bank Erosion 1977–1979: Red Bluff, California, California Department of Water Resources, Northern District, 58 p.

Camporeale, C., Perona, P., Porporato, A., and Ridolfi, L., 2005, On the long-term behavior of meandering rivers:

Water Resources Research, v. 41, p. W12403, doi: 10.1029/2005WR004109.

Chen, D., and Duan, J.G., 2006, Modeling width adjustment in meandering channels: Journal of Hydrology (Amsterdam), v. 321, p. 59–76, doi: 10.1016/j.jhydrol.2005.07.034.

Constantine, C.R., 2006, Quantifying the Connections between Flow, Bar Deposition, and Meander Migration in Large Gravel-Bed Rivers [Ph.D. thesis]: Santa Barbara, University of California, 202 p.

Constantine, J.A., and Dunne, T., 2008, Meander cutoff and the controls on the production of oxbow lakes: Geology, v. 36, p. 23–26, doi: 10.1130/G24130A.1.

Dietrich, W.E., and Smith, J.D., 1983, Influence of the point bar on flow through curved channels: Water Resources Research, v. 19, p. 1173–1192, doi: 10.1029/WR019i005p01173.

Dietrich, W.E., Smith, J.D., and Dunne, T., 1979, Flow and sediment transport in a sand bedded meander: The Journal of Geology, v. 87, p. 305–315.

Engelund, F., 1974, Flow and bed topography in channel bends: Journal of the Hydraulics Division, v. 100, p. 1631–1648.

Fagherazzi, S., Gabet, E.J., and Furbish, D.J., 2004, The effect of bidirectional flow on tidal channel planforms: Earth Surface Processes and Landforms, v. 29, p. 295–309, doi: 10.1002/esp.1016.

Farid, A., Goodrick, D.C., and Sorroshian, S., 2006, Using airborne lidar to discern age classes of cottonwood trees in a riparian area: Western Journal of Applied Forestry, v. 21, p. 149–158.

Fisk, H.N., 1947, Fine-Grained Alluvial Deposits and Their Effects on Mississippi River Activity, Volumes 1 & 2: Vicksburg, Mississippi, Mississippi River Commission, 84 p.

Fuller, I.C., Large, A.R.G., and Milan, D.J., 2003, Quantifying channel development and sediment transfer following chute cutoff in a wandering gravel-bed river: Geomorphology, v. 54, p. 307–323, doi: 10.1016/S0169-555X(02)00374-4.

Furbish, D.J., 1988, River-bend curvature and migration: How are they related?: Geology, v. 16, p. 752–755, doi: 10.1130/0091-7613(1988)016<0752:RBCAMH>2.3.CO;2.

Furbish, D.J., 1991, Spatial autoregressive structure in meander evolution: Geological Society of America Bulletin, v. 103, p. 1576–1589, doi: 10.1130/0016-7606(1991)103<1576:SASIME>2.3.CO;2.

Gagliano, S.M., and Howard, P.G., 1984, The neck cutoff oxbow lake cycle along the Lower Mississippi River, *in* Elliot, C.M., ed., River Meandering: New York, American Society of Civil Engineers, p. 147–158.

Gay, G.R., Gay, H.H., Gay, W.H., Martinson, H.A., Meade, R.H., and Moody, J.A., 1998, Evolution of cutoffs across meander necks in Powder River, Montana, USA: Earth Surface Processes and Landforms, v. 23, p. 651–662, doi: 10.1002/(SICI)1096-9837(199807)23:7<651::AID-ESP891>3.0.CO;2-V.

Gran, C., and Paola, C., 2001, Riparian vegetation controls on braided stream dynamics: Water Resources Research, v. 37, p. 3275–3283, doi: 10.1029/2000WR000203.

Griggs, F.T., and Golet, G.H., 2002, Riparian valley oak (*Quercus lobata*) forest restoration on the Middle Sacramento River, California: U.S. Department of Agriculture Forest Service General Technical Report PSW-GTR-184, p. 543–550.

Harris, R.R., 1987, Occurrence of vegetation on geomorphic surfaces in the active floodplain of a California alluvial stream: American Midland Naturalist, v. 118, p. 393–405, doi: 10.2307/2425796.

Hauer, C., and Habersack, H., 2009, Morphodynamics of a 1000-year flood in the Kamp River, Austria, and impacts on floodplain morphology: Earth Surface Processes and Landforms, v. 34, p. 654–682, doi: 10.1002/esp.1763.

Hickin, E.J., 1974, The development of meanders in natural river channels: American Journal of Science, v. 274, p. 414–442.

Hickin, E.J., and Nanson, G.C., 1975, The character of channel migration on the Beatton River, northeast British Colombia, Canada: Geological Society of America Bulletin, v. 86, p. 487–494, doi: 10.1130/0016-7606(1975)86<487:TCOCMO>2.0.CO;2.

Hooke, J.M., 1995, River channel adjustment to meander cutoffs on the River Bollin and River Dane, northwest England: Geomorphology, v. 14, p. 235–253, doi: 10.1016/0169-555X(95)00110-Q.

Hooke, J.M., and Redmond, C.E., 1992, Causes and nature of river planform change, *in* Billi, P., Hey, R.D., Thorne, C.R., and Tacconi, P., eds., Dynamics of Gravel-Bed Rivers: New York, John Wiley & Sons, p. 557–571.

Howard, A.D., 1992, Modeling channel migration and floodplain sedimentation in meandering streams, *in* Carling, P.A., and Petts, G.E., eds., Lowland Floodplain Rivers: New York, John Wiley & Sons, p. 1–42.

Howard, A.D., 1996, Modelling channel evolution and floodplain morphology, *in* Anderson, M.G., Walling, D.E., and Bates, P.D., eds., Floodplain Processes: New York, John Wiley & Sons, p. 15–62.

Howard, A.D., and Knutson, T.R., 1984, Sufficient conditions for river meandering: A simulation approach: Water Resources Research, v. 20, p. 1659–1667, doi: 10.1029/WR020i011p01659.

Hupp, C.R., and Osterkamp, W.R., 1996, Riparian vegetation and fluvial geomorphic processes: Geomorphology, v. 14, p. 277–295, doi: 10.1016/0169-555X(95)00042-4.

Ikeda, S., 1989, Sediment transport and sorting at bends, *in* Ikeda, S., and Parker, G., eds., River Meandering: American Geophysical Union Water Resources Monograph 12, p. 103–126.

Ikeda, S., Parker, G., and Sawai, K., 1981, Bend theory of river meanders: Part 1. Linear development: Journal of Fluid Mechanics, v. 112, p. 363–377, doi: 10.1017/S0022112081000451.

Johannesson, H., and Parker, G., 1988, Inertial Effects of Secondary and Primary Flow in Curved Channels: St. Anthony Falls Hydraulic Laboratory External Memorandum 208, University of Minnesota, 35 p.

Johannesson, H., and Parker, G., 1989, Linear theory of river meanders, *in* Ikeda, S., and Parker, G., eds., River Meandering: American Geophysical Union Water Resources Monograph 12, p. 181–214.

Kean, J.W., and Smith, J.D., 2005, Generation and verification of theoretical rating curves in the Whitewater River basin, Kansas: Journal of Geophysical Research, v. 110, p. F04012, doi: 10.1029/2004JF000250.

Keller, E.A., and Swanson, F.J., 1979, Effects of large organic material on channel form and fluvial processes: Earth Surface Processes, v. 4, p. 361–380, doi: 10.1002/esp.3290040406.

Kikkawa, H., Ikeda, S., and Kitagawa, A., 1976, Flow and bed topography in curved open channels: Journal of the Hydraulics Division, v. 102, p. 1327–1342.

Knight, D.W., and Shiono, K., 1996, River channel and floodplain hydraulics, *in* Anderson, M.G., Walling, D.E., and Bates, P.D., eds., Floodplain Processes: New York, John Wiley & Sons, p. 139–181.

Lauer, J.W., and Parker, G., 2008, Net local removal of floodplain sediment by river meander migration: Geomorphology, v. 96, p. 123–149, doi: 10.1016/j.geomorph.2007.08.003.

Leliavsky, S., 1966, An Introduction to Fluvial Hydraulics: New York, Dover Publications, Inc., 257 p.

Lewis, G.W., and Lewin, J., 1983, Alluvial cutoffs in Wales and Borderlands, *in* Collinson, J.D., and Lewin, J., eds., Modern and Ancient Fluvial Systems: International Association of Sedimentologists Special Publication 6, p. 145–154.

Luhar, M., Rominger, J., and Nepf, H., 2008, Interaction between flow, transport and vegetation spatial structure: Environmental Fluid Mechanics, v. 8, p. 423–439, doi: 10.1007/s10652-008-9080-9.

Mackin, J.H., 1956, Causes of braiding by a graded river: Geological Society of America Bulletin, v. 67, p. 1717–1718.

Markham, A.J., and Thorne, C.R., 1992, Geomorphology of gravel-bed river bends, *in* Billi, P., Hey, R.D., Thorne, C.R., and Tacconi, P., eds., Dynamics of Gravel-Bed Rivers: New York, John Wiley & Sons, p. 433–456.

Micheli, E.R., Kirchner, J.W., and Larsen, E.W., 2004, Quantifying the effect of riparian forest versus agricultural vegetation on river meander migration rates, central Sacramento River, California, USA: River Research and Applications, v. 20, p. 537–548, doi: 10.1002/rra.756.

Millar, R.G., 2000, Influence of bank vegetation on alluvial channel patterns: Water Resources Research, v. 36, p. 1109–1118, doi: 10.1029/1999WR900346.

Murray, A.B., and Paola, C., 2003, Modelling the effect of vegetation on channel pattern in bedload rivers: Earth Surface Processes and Landforms, v. 28, p. 131–143, doi: 10.1002/esp.428.

Nelson, J.M., Bennett, J.P., and Wiele, S.M., 2003, Flow and sediment-transport modeling, *in* Kondolf, G.M., and Piégay, H., eds., Tools in Fluvial Geomorphology: Sussex, UK, John Wiley & Sons, p. 539–576.

Nepf, H.M., 1999, Drag, turbulence, and diffusion in flow through emergent vegetation: Water Resources Research, v. 35, p. 479–489, doi: 10.1029/1998WR900069.

Nicholas, A.P., and McLelland, S.J., 2004, Computational fluid dynamics modelling of three-dimensional processes on natural river floodplains: Journal of Hydraulic Research, v. 42, p. 131–144.

Norris, R.M., and Webb, R.W., 1976, Geology of California: New York, John Wiley & Sons, 365 p.

Odgaard, A.J., 1987, Streambank erosion along two rivers in Iowa: Water Resources Research, v. 23, p. 1225–1236, doi: 10.1029/WR023i007p01225.

Parker, G., and Andrews, E.D., 1986, On the time development of meander bends: Journal of Fluid Mechanics, v. 162, p. 139–156, doi: 10.1017/S0022112086001970.

Perucca, E., Camporeale, C., and Ridolfi, L., 2007, Significance of the riparian vegetation dynamics on meandering river morphodynamics: Water Resources Research, v. 43, p. W03430, doi: 10.1029/2006WR005234.

Pizzuto, J.E., and Meckelnburg, T.S., 1989, Evaluation of a linear bank erosion equation: Water Resources Research, v. 25, p. 1005–1013, doi: 10.1029/WR025i005p01005.

Rowland, D.L., Biagini, B., and Evans, A.S., 2000, Variability among five riparian cottonwood (*Populus fremontii* Wats.) populations: An examination of size, density, and spatial distribution: Western North American Naturalist, v. 60, p. 384–393.

Sedgwick, J.A., and Knopf, F.L., 1986, Cavity-nesting birds and the cavity-tree resource in plains cottonwood bottomlands: The Journal of Wildlife Management, v. 50, p. 247–252, doi: 10.2307/3801906.

Sellin, R.H.J., and Willetts, B.B., 1996, Three-dimensional structures, memory and energy dissipation in meandering compound flow, *in* Anderson, M.G., Walling, D.E., and Bates, P.D., eds., Floodplain Processes: New York, John Wiley & Sons, p. 255–297.

Sellin, R.H.J., Ervine, D.A., and Willetts, B.B., 1993, Behaviour of meandering two-stage channels: Proceedings of the Institute of Civil Engineers: Water Maritime and Energy, v. 101, p. 99–111, doi: 10.1680/iwtme.1993.23591.

Shiono, K., and Muto, Y., 1998, Complex flow mechanisms in compound meandering channels with overbank flow: Journal of Fluid Mechanics, v. 376, p. 221–261, doi: 10.1017/S0022112098002869.

Simon, A., and Collison, J.C., 2002, Quantifying the mechanical and hydrologic effects of riparian vegetation on streambank stability: Earth Surface Processes and Landforms, v. 27, p. 527–546, doi: 10.1002/esp.325.

Singer, M.B., 2008, A new sampler for extracting bed material sediment from sand and gravel beds in navigable rivers: Earth Surface Processes and Landforms, v. 33, 2277–2284, doi: 10.1002/esp.1661.

Singer, M.B., and Dunne, T., 2001, Identifying eroding and depositional reaches of valley by analysis of suspended sediment transport in the Sacramento River, California: Water Resources Research, v. 37, p. 3371–3381, doi: 10.1029/2001WR000457.

Singer, M.B., and Dunne, T., 2004a, Modeling decadal bed-material sediment flux based on stochastic hydrology: Water Resources Research, v. 40, no. W03302, doi: 10.1029/2003WR002723.

Singer, M.B., and Dunne, T., 2004b, An empirical-stochastic, event-based program for simulating inflow from a tributary network: Framework and application to the Sacramento River basin, California: Water Resources Research, v. 40, no. W07506, doi: 10.1029/2003WR002725.

Slingerland, R., and Smith, N.D., 1998, Necessary conditions for a meandering-river avulsion: Geology, v. 26, p. 435–438, doi: 10.1130/0091-7613(1998)026<0435:NCFAMR>2.3.CO;2.

Smith, J.D., 2004, The role of riparian shrubs in preventing floodplain unraveling along the Clark Fork of the Columbia River in Deer Lodge Valley, Montana, *in* Bennett, S.J., and Simon, A., eds., Riparian Vegetation and Fluvial Geomorphology: Washington, D.C., American Geophysical Union, p. 71–85.

Stein, O.R., and LaTray, D.A., 2002, Experiments and modeling of head cut migration in stratified soils: Water Resources Research, v. 38, no. WR001166, doi: 10.1029/2001WR001166.

Stølum, H., 1996, River meandering as a self-organization process: Science, v. 271, p. 1710–1713, doi: 10.1126/science.271.5256.1710.

Stølum, H., 1998, Planform geometry and dynamics of meandering rivers: Geological Society of America Bulletin, v. 110, p. 1485–1498, doi: 10.1130/0016-7606(1998)110<1485:PGADOM>2.3.CO;2.

Sun, T., Meakin, P., and Jøssang, T., 1996, A simulation model for meandering rivers: Water Resources Research, v. 32, p. 2937–2954, doi: 10.1029/96WR00998.

Tal, M., and Paola, C., 2007, Dynamic single-thread channels maintained by the interaction of flow and vegetation: Geology, v. 35, p. 347–350, doi: 10.1130/G23260A.1.

Thompson, D.M., 2003, A geomorphic explanation for a meander cutoff following channel relocation of a coarse-bedded river: Environmental Management, v. 31, p. 385–400, doi: 10.1007/s00267-002-2842-0.

Thorne, C.R., and Hey, H.D., 1979, Direct measurements of secondary currents at a river inflection point: Nature, v. 280, p. 226–228, doi: 10.1038/280226a0.

Thorne, C.R., Zevenbergen, L.W., Pitlick, J.C., Rais, S., Bradley, J.B., and Julien, P.Y., 1985, Direct measurements of secondary currents in a meandering sand-bed river: Nature, v. 315, p. 746–747, doi: 10.1038/315746a0.

White, B.L., and Nepf, H.M., 2008, A vortex-based model of velocity and shear stress in a partially vegetated shallow channel: Water Resources Research, v. 44, no. W01412, doi: 10.1029/2006WR005651.

Whiting, P.J., and Dietrich, W.E., 1991, Convective accelerations and boundary shear stress over a channel bar: Water Resources Research, v. 27, p. 783–796, doi: 10.1029/91WR00083.

Wilson, C.A.M.E., and Horritt, M.S., 2002, Measuring the flow resistance of submerged grass: Hydrological Processes, v. 16, p. 2589–2598, doi: 10.1002/hyp.1049.

Wormleaton, P.R., Sellin, R.H.J., Bryant, T., Loveless, J.H., Hey, R.D., and Catmur, S.E., 2004, Flow structures in a two-stage channel with a mobile bed: Journal of Hydraulic Research, v. 42, p. 145–162.

Wright, S.A., and Schoellhamer, D.H., 2004, Trends in the sediment yield of the Sacramento River, California, 1957–2001: San Francisco Estuary & Watershed Science, v. 2, no. 2, p.1–14.

Zimmerman, C., and Kennedy, J.F., 1978, Transverse bed slopes in curved alluvial streams: The Journal of the Hydraulics Division: Proceedings of the American Society of Civil Engineers, v. 104, p. 33–48.

Zolezzi, G., and Seminara, G., 2001, Upstream influence in erodible beds: Physics and Chemistry of the Earth. Part B: Hydrology, Oceans and Atmosphere, v. 26, p. 65–70, doi: 10.1016/S1464-1909(01)85016-4.

Manuscript Received 4 October 2008
Revised Manuscript Received 14 April 2009
Manuscript Accepted 26 April 2009

Printed in the USA